Si-Mo-MODIFIED ALUMINIDE SLURRY COATING FOR HIGH TEMPERATURE PROTECTION OF AUSTENITIC STAINLESS STEEL

Syamimi Abu Kassim[1], Nur Muzirah Md Shukri[1], Syazana Ahmad Zubir[1], Anasyida Abu Seman[1] and Tuti Katrina Abdullah[1*]

[1]School of Materials and Minerals Resources Engineering, Engineering Campus, Universiti Sains Malaysia, Seri Ampangan, Seberang Perai Selatan, 14300 Nibong Tebal, Pulau Pinang, Malaysia.

*tutikatrina@usm.my

Abstract. Slurry aluminide coating is considered one of the most excellent coating materials to enhance hot corrosion resistance for high temperature applications. In this research, Si-, Mo- and Si-Mo-modified slurry aluminide coatings were prepared on 304 stainless steel at 650 ºC for 4 h and 6 h. The influence of Si, Mo and Si-Mo additions into the coatings was studied by comparing the coating properties at different aluminizing time. The physical, chemical and mechanical properties of the aluminide coatings were characterized using the Vickers microhardness test, FESEM, EDX and XRD. The addition of Si and Mo into the coating slightly changes the coating behaviour of the alloy. A multi-layered coating structure was observed after the aluminizing for all coating samples. A dense and continuous inner layer made up of FeAl-base intermetallic is believed to improve the corrosion resistance of the stainless steel. The hardness value (HV) increased with an increasing in aluminizing time for Mo- and Si-modified aluminide coatings. In contrast, Si-Mo-modified aluminide coating showed a decreased in hardness value (HV) due to the formation of multi-crack and porous coating structures. A modified slurry aluminide coatings on 304 stainless steel could be considered as a viable potential for high temperature application.

Keywords: Aluminide coating, Aluminizing, Si-Mo-modified, Austenitic stainless steel, High-temperature protection

Article Info

Received 6th October 2021
Accepted 5th December 2021
Published 20th December 2021

ISSN: 1823-7010, eISSN: 2600-7444

Introduction

Ferritic and austenitic stainless steel has been extensively used for high temperature applications, such as superheaters, boilers, and power plants reactors due to a good compromise in corrosion resistance, high temperature mechanical properties and cost-effective materials [1-4]. However, the oxidation resistance of stainless steel became limited at a high operating temperature between 620 ºC - 650 ºC due to the formation of a layered and less protective Fe_3O_4 and Cr-rich spinel on the steel surfaces [5,6]. This condition will affect the lifecycle cost of the material components. Surface treatment, such as high temperature coating has been proposed by researchers to improve the oxidation resistance of stainless steel under hot corrosion conditions. Among all the high temperature coatings, aluminide coating is the most widely used [7]. Aluminide coating has a great potential for protecting the alloys from corrosion damages because of its ability to grow protective scales. The commonly used preparation methods for aluminide coating are slurry aluminizing, Al-electroplating, hot dipping aluminizing (HDA), electrochemical deposition (ECD), powder embedded aluminizing (PEA), pack cementation (PC), physical vapour deposition (PVD), chemical vapour deposition (CVD), etc. [9-12]. However, an interest in slurry aluminizing coating has increased due to process simplicity, cost efficiency, environmental friendly and high coating flexibility [13].

During thermal exposure, a layer of Al_2O_3 was developed on the steel surfaces after aluminizing in the oxidizing atmosphere [8-9]. The formation of the alumina layer on the coating surface can prevent further destruction of the substrate in a high temperature corrosive environment [8]. The formation of Al_2O_3-base coating is also believed to significantly increase the corrosion resistance of iron-based alloy [13]. Unfortunately, flaws in the mechanical properties such as cracks may be formed during the deposition or long-term exposure of the coating, resulting from a mismatch in the thermal expansion coefficient (CTE) between the coating and alloy substrate [6]. The mechanical properties of the aluminized steel decrease at elevated temperatures due to the depletion of aluminium, which is caused by the interdiffusion of aluminium from the coating into the alloy substrate [6]. This factor becomes a challenge in developing a protective aluminide coating layer. Moreover, the Al_2O_3 layer formed on the coating surface could easily spall during cyclic oxidation exposure [15].

Currently, numerous works are focused on modifying the aluminide coating with an addition of a few alloying elements to acquire good oxidation and hot corrosion resistance [16]. Alloying elements, such as Cr, Si, Pt, Zr, Ce and Mo-doped aluminide coating have been demonstrated to be beneficial against hot corrosion resistance [17-20]. The addition of Si in the aluminide coating was reported by Zarei et al. (2020) to improve the protective properties of the forming oxide layer at high temperatures due to the formation of Al_2O_3-SiO_2 layer. According to the study, the modified coating could change the degradation mechanism of the protective surface oxide layer from spallation to a nodular growth mechanism [20]. A well-modified aluminide coating is important to the development of iron-based alloy with higher resistance against a harsh environment. The addition of fair amounts of Si and Mo in aluminide coating could help in improving the coating performance and extend the corrosion resistance of the alloy.

A comparative study on the effect of Si and Mo addition on the properties of slurry aluminide coating has not yet been clarified. Furthermore, no studies have yet been reported on Mo-modified aluminide coating for high temperature application. Therefore, this work

was purposely conducted to investigate the microstructure, chemical composition and mechanical properties of the aluminide coating at different time exposures and different coating compositions. The study is focused on the effect of alloying elements on microstructure transformation, intermetallic layer thickness, phase's constitution and coating hardness of the aluminide coatings. The results would be beneficial on a development of a new coating for high temperature applications.

Materials and Methods

A plate-shaped of 304 stainless steel (HH Saintifik Ent.) was cut using a hydraulic cutting machine into 10 mm x 10 mm x 0.15 mm dimensions. The chemical composition of the 304 stainless steel is given in Table 1. The alloy samples were ground to 320 grit using SiC paper before the coating. The aluminide coating was deposited using a slurry aluminizing technique. The coating slurry was prepared by mixing 57 wt. % of the organic binder (distilled water and polyvinyl alcohol) and 43 wt.% of the solute mixture. Three different types of solute compositions were used in this study as listed in Table 2. A slurry mixture was sprayed on the surfaces of 304 stainless steel using a spray gun (Suniw model K-3), then dried in laboratory air before solidifying at 400 ºC for 1 h to allow the removal of the binder followed by aluminizing process. The aluminizing process was carried out at 650 ºC [21–24] for 4 h and 6 h [25–28] under a flow of argon gas (1 atm) with a heating rate of 10°C/min. The morphology and elemental distribution of all coated samples were characterized using a field emission scanning electron microscopy (FESEM; Zeiss Supra 35 VP system) equipped with energy dispersive X-ray spectroscopy (EDX; Edax Ametex Z2 analyzer). The samples were inspected in secondary electron (SE) mode for surface morphology and backscattered electron (BSE) mode for cross-section morphology. Phase identification of coated samples was carried out using X-ray diffraction (XRD, Bruker Advanced D8) with Cu Kα radiation (λ = 0.15406 nm) and 2θ scanning from 10° to 90°. Vickers microhardness (LECO micro-indentation hardness tester LM248AT) test was performed on the coated samples using a square diamond indenter with a load of 0.2 N to evaluate the mechanical properties of the coating layer.

Table 1. Chemical composition of as-received 304 stainless steel

Elements	Fe	Cr	Ni	Mn	Si	Cu	Mo	Co	V
wt. %	Bal.	17.90	8.28	0.84	0.5	0.23	0.19	0.18	0.10

Table 2. The ratio of solute composition of slurry aluminide coating

Element coatings	Solute composition (wt. %)		
	Al	Si	Mo
Si-modified aluminide coating	33.00	10.00	0.00
Mo-modified aluminide coating	33.00	0.00	10.00
Si-Mo-modified aluminide coating	33.00	5.00	5.00

Results and Discussion

Physical and chemical properties of the coatings. The performance of the developed coating was largely dependent on the coating microstructure and its chemical composition

[29]. Figure 1 presents the surface (SE) and cross-sectional (BSE) morphology of the 304 stainless steel after aluminizing at 650 °C for 4 h and 6h. The surface morphology of the modified coating after aluminizing mostly showed a mixture of granules, cylindrical-like and hollow colloid structures. A least significant difference in the surface morphologies was observed for all samples with modified coating as shown in Figures 1(a) - 1(f). Both Al-Si-modified and Al-Mo-modified coatings revealed the coating surfaces grew denser as the aluminizing time increased to 6 h. However, Al-Si-Mo-modified coating showed the opposite morphology behaviour relative to Al-Si-modified and Al-Mo-modified coatings as the aluminizing time increases. The size and distribution of hollow structures on the Al-Si-Mo-modified coating surface increased with an increase in aluminizing time (Figure 1(f)). EDX area and EDX spot analysis on aluminide-coated 304 stainless steel are listed in Table 3. EDX area analysis revealed the surface of all modified aluminide coatings was mostly composed of Al-rich oxides (area 1- 6).

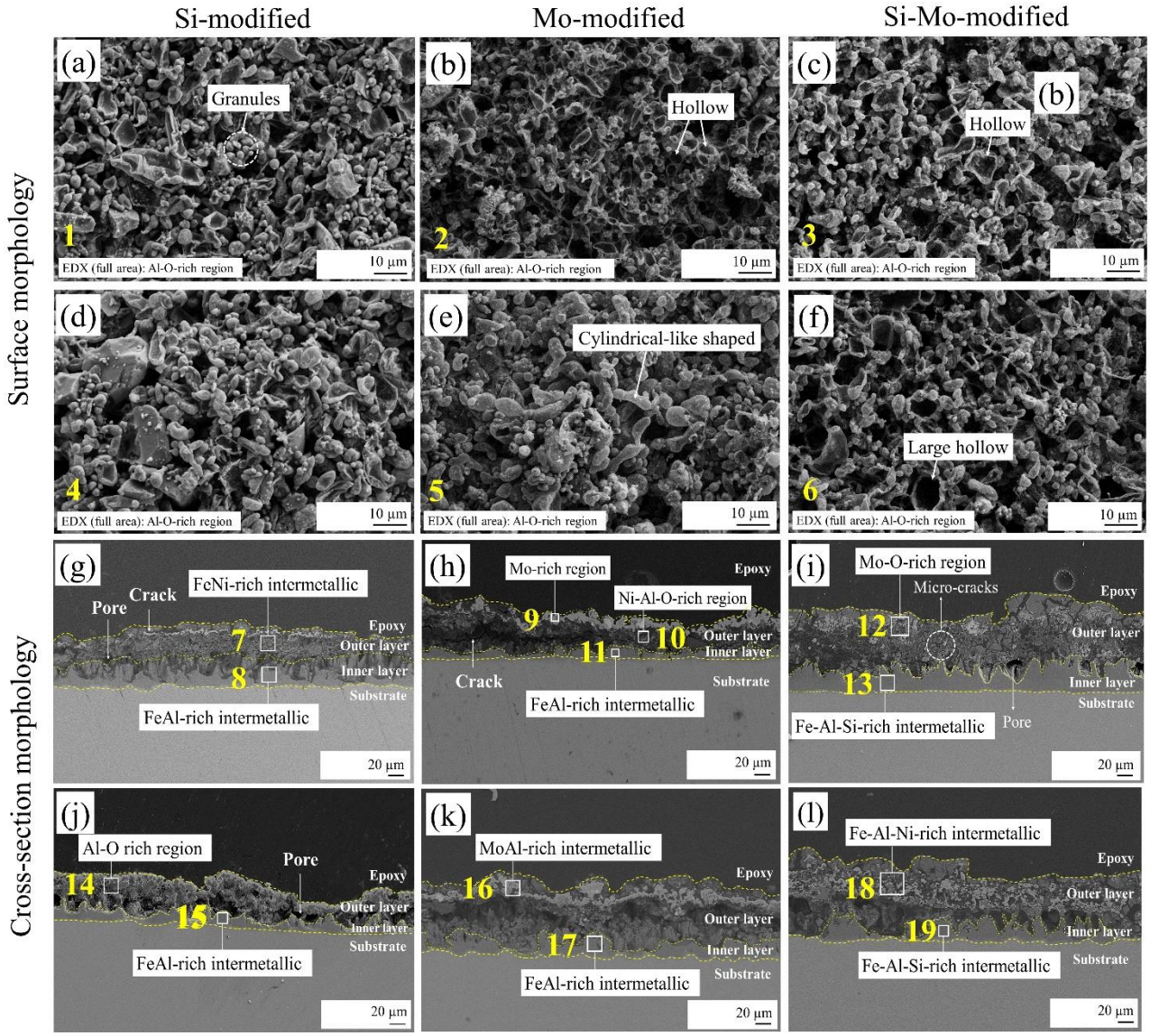

Figure 1. FESEM micrographs obtained on modified aluminide coatings after aluminizing at 650 ºC for 4 h (surface morphology: (a) - (c) at 1000x magnification and cross-section morphology: (g) - (i) at 250x magnification) and 6 h (surface morphology: (d) - (f) at 1000x magnification and cross-section morphology: (j) - (l) at 250x magnification

The FESEM cross-section morphologies of aluminide coatings on 304 stainless steel are respectively shown in Figures 1(g) – 1(l). The modified aluminide coatings achieved a two-layered structure by showing: i. an outer layer with multi-cracks and a rough structure called diffusion zone, and ii. a dense and homogenous inner layer called intermetallic layer or interdiffusion layer. The inner interdiffusion layer was well adhered to the substrate alloy. The presence of porosities can also be observed between the inner and outer coating layers, while cracks only present on the outer surface of the coatings. However, the cracks do not penetrate into the inner interdiffusion layer coatings. The different structure of cracks and pores on the surface of the coatings are normally attributed to the mismatch between different thermal expansion coefficients and metallurgical phases [2,30].

Table 3. EDX data analysis on surface (area 1 - 6) and cross section (spot 7 -19) of 304 stainless steel after aluminizing at 650 ºC for 4 h and 6 h.

Aluminizing time (h)	EDX area/spot	Elements (wt. %)						
		O	Fe	Al	Si	Mo	Ni	Cr
4	**1**	19.48	0.46	62.60	17.46	0.00	0.00	0.00
	2	30.75	0.44	61.26	0.00	7.55	0.00	0.00
	3	29.76	1.50	62.02	2.57	4.15	0.00	0.00
6	**4**	28.58	0.64	63.02	7.76	0.00	0.00	0.00
	5	33.10	1.75	58.15	0.00	7.00	0.00	0.00
	6	31.58	0.68	58.38	3.14	6.22	0.00	0.00
4	**7**	0.72	46.51	0.78	0.24	0.00	51.75	0.00
	8	1.18	25.39	60.38	9.60	0.00	3.45	0.00
	9	3.78	3.76	0.65	0.00	87.09	4.72	0.00
	10	35.18	4.74	27.86	0.00	5.60	26.62	0.00
	11	3.09	44.80	46.43	0.00	2.52	3.16	0.00
	12	10.26	0.77	1.50	0.98	79.63	6.86	0.00
	13	1.36	10.79	67.81	13.20	6.84	0.00	0.00
6	**14**	18.13	6.40	65.72	5.83	0.00	3.92	0.00
	15	2.94	31.15	52.41	8.61	0.00	4.89	0.00
	16	2.28	3.17	44.55	0.00	45.85	4.15	0.00
	17	1.98	38.63	53.48	0.00	1.49	4.42	0.00
	18	3.34	18.87	52.12	8.17	0.00	17.50	0.00
	19	1.50	32.02	48.92	12.83	0.00	4.73	0.00

According to the EDX profiles of Al-Si-modified aluminide coating on the 304 stainless steel, the outer coating layer consists of high amount of Fe and Ni (FeNi-rich layer). This occurs after 4 h of aluminizing time (spot 7). Ni content in the outer layer reduced after 6 h of aluminizing, whereas, the Fe and Al content were conversely higher (spot 8). In the outer layer of Al-Mo-modified aluminide coating, the light grey layer consists of a high amount of Mo (spot 9), while the dark grey region has a high amount of Ni, Al and O (spot 10). The inner interdiffusion layer of both Al-Si-modified and Al-Mo-modified coating alloys detected a high amount of Fe and Al (FeAl-rich layer) in EDX spot 8 and spot 11. The formation of the FeAl-base coating layer resulted from the inward diffusion of aluminium and outward diffusion of iron [30]. FeAl-intermetallic phases that formed during aluminizing of Fe-based alloy could enhance the corrosion resistance of the alloy. [31]. As for Al-Si-Mo-modified coating alloy, the outer region of the coating layer after 4 h of aluminizing was composed of Mo-rich oxides (spot 12). Then, a FeAlNi-rich layer was detected at the outer

coating after 6 h of aluminizing. The EDX scan on the inner interdiffusion layer of Al-Si-Mo-modified coating revealed the coating consisted of FeAlSi-rich layer (spot 13 and spot 19). This finding proves that the addition of Si to aluminum not only alters the microstructure of the aluminide layer but also transforms the intermetallic compound of Fe-Al into Fe-Al-Si [32].

The X-ray diffraction patterns of all modified aluminide coating samples are shown in Figure 2. Figures 2(a) and 2(b) show that the XRD analysis on both Al-Si-modified coatings consists of Al, $FeAl_3$, Fe_2Al_5, Al_7Fe_2Si, SiO_2 and Al_2O_3 phases. The dominant phases of the coating layer were Fe_2Al_5 and Al_7Fe_2Si. A minor peak of SiO_2 was detected in the diffractogram. According to Tavakoli et al. (2020), the presence of SiO_2 phases on the coating layer also contributed to a higher corrosion resistance [16]. Meanwhile, Al, Mo, MoO_3, $FeAl_3$ and Fe_2Al_5 were detected by XRD analysis on the Al-Mo-modified coating after aluminizing (Figures 2(c) and 2(d)). The XRD analysis indicates the main phases of the coating layer were the MoO_3 and Fe_2Al_5 phases.

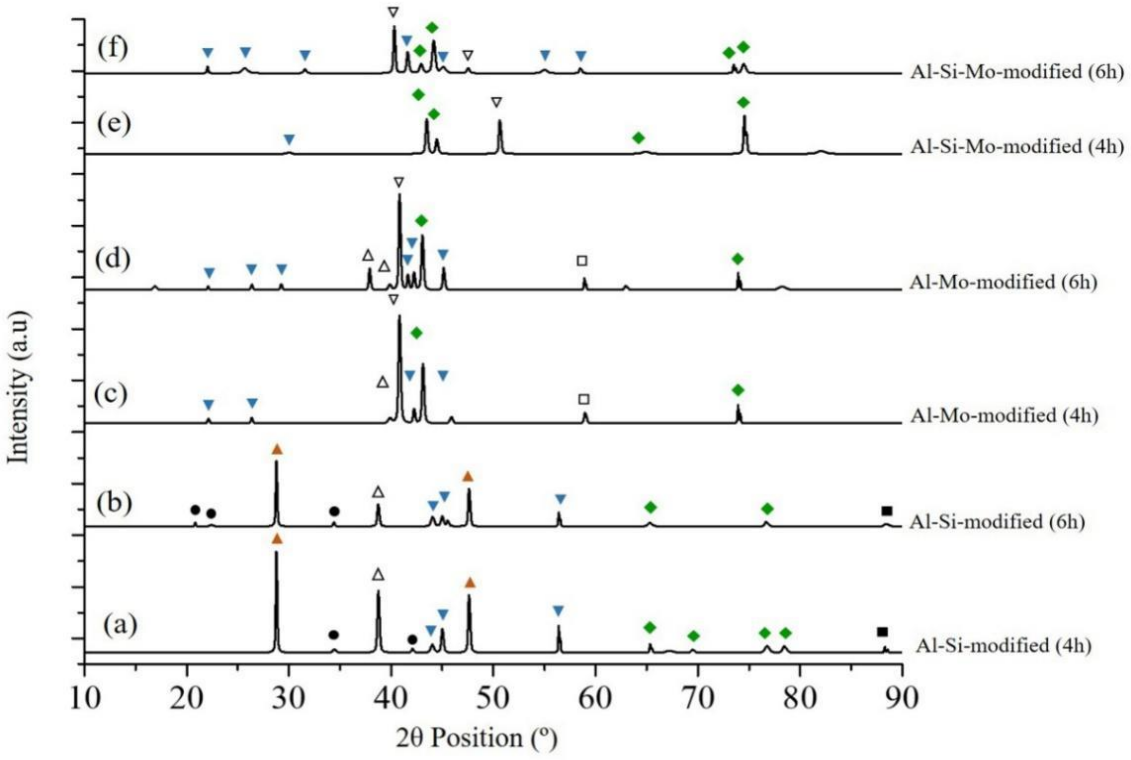

Samples	XRD phases
Al-Si 4h	Al, $FeAl_3$, Fe_2Al_5, Al_7Fe_2Si, Al_2O_3, SiO_2
Al-Si 6 h	Al, $FeAl_3$, Fe_2Al_5, Al_7Fe_2Si, Al_2O_3, SiO_2
Al-Mo 4h	Al, Mo, MoO_3, $FeAl_3$, Fe_2Al_5
Al-Mo 6h	Al, Mo, MoO_3, $FeAl_3$, Fe_2Al_5
Al-Si-Mo 4h	$FeAl_3$, Fe_2Al_5, MoO_3
Al-Si-Mo 6h	$FeAl_3$, Fe_2Al_5, MoO_3

▲ = Al_7Fe_2Si ▼ = $FeAl_3$
◆ = Fe_2Al_5 ● = SiO_2
■ = Al_2O_3 ▽ = MoO_3
△ = Al □ = Mo

Figure 2. XRD patterns of all modified aluminide-coated 304 stainless steel

Another XRD result on Al-Si-Mo-modified coating showed that the aluminide coating layer was mainly composed of Fe_2Al_5, $FeAl_3$ and MoO_3. The dominant phase of the coatings detected was MoO_3 (Figures 2(e) and 2(f)). The phases of Fe_2Al_5 and $FeAl_3$ may be formed through the iron-aluminium reaction [9,14]. Fe_2Al_5 phase was firstly formed with a rapid infiltration of Al atom disclosed to the substrate layer (equation 1). Fe_2Al_5 then reacted with Fe or Al atoms to form $FeAl_3$ or FeAl phases according to equations 2-3.

$$2\,Fe + 5Al = Fe_2Al_5 \quad (1)$$

$$Fe_2Al_5 + Al = 2\,FeAl_3 \quad (2)$$

$$Fe_2Al_5 + 3Fe = 5FeAl \quad (3)$$

According to Dong et al. (2019), among all of the FeAl-base phases, the Fe_2Al_5 phase exhibited the best growth kinetic condition with a fast-growing rate followed by $FeAl_3$ and FeAl as the slowest phase-growing rate. According to Chang et al. (2006), Si can also be dissolved in FeAl, $FeAl_2$, Fe_2Al_5 and $FeAl_3$, leading to the precipitation of FeAl(Si, Cr) [33], which might be the reason for the presence of Al_7Fe_2Si phase detected in XRD diffractogram. According to Zarei et al. (2020), Al_7Fe_2Si intermetallic compound was mostly formed in the joint interface of AlSi intermetallic and steel. However, the formation of Al_7Fe_2Si was considered to be lower than Fe_2Al_5 and $FeAl_3$ [14,20]. Cheng and Wang (2009) stated that FeAlSi intermetallic compounds usually formed with two phases of Al_7Fe_2Si and $(Al, Si)_5Fe$, which precipitated in FeAl intermetallic layer. The presence of $(Al, Si)_5Fe$ phases on aluminized steel was infrequently reported due to the difficulties in detecting the phase by XRD [34].

The outward diffusion of Fe and Ni from the matrix was also identified as contributing to the main phases of the coating, as confirmed through XRD. As related to EDX spot 10, high Ni, Al and O elements distribution spotted at the outer layer of Al-Mo-modified coating can be related to $NiAl_2O_4$ formation. According to Targhi et al. (2020), the $NiAl_2O_4$ phase reflects very mild coating destruction on a surface of aluminide coating [16]. Meanwhile, MoO_3 is a volatile species and might evaporate from the coating surfaces, leaving a porous and hollow coating layer that leads to oxidation failure [35]. The volatilization of MoO_3 prevents a dense coating layer to be formed. These loose oxidation layers provide a pathway of oxygen diffusion, which later causes simultaneous oxidation of metallic elements in the layer.

The overall thickness measurement of the coating layer is shown in Figure 3. Al-Si-modified and Al-Si-Mo-modified coatings on the 304 stainless steel after 4 h of aluminizing revealed the thickness of the coating was 66.06 µm (inner: 33.30 ± 4.53 µm + outer: 32.76 ± 7.59 µm) and 95.47 µm (inner: 26.09 ± 6.96 µm + outer: 69.38 ± 12.54 µm), respectively (Figures 3(a) and 3(b)). The coating layer thickness inversely changes with aluminizing time. As the aluminizing time increased to 6 h, the thickness of the inner coating layer reduced. The thickness of Al-Si-modified and Al-Si-Mo-modified coatings reduced to 52.05 µm (inner: 13.90 ± 4.79 µm + outer: 38.15 ± 10.19 µm) and 80.75 µm (inner: 15.79 ± 7.98 µm + outer: 64.96 ± 17.43 µm), respectively. The reduction in layer thickness was attributed to the inward diffusion of Al/Si/Mo and the outward growth of the aluminide coating layer. The outward diffusion of Fe from alloy substrate into FeAl-base intermetallic led to the precipitation of Al_7Fe_2Si phase as shown in the previous XRD diffractogram. According to Zarei et al. (2020), the decrease in the thickness of the intermetallic layer was related to the occupancy of Al vacancies in the Fe_2Al_5 by Si atom, causing a slower growth rate of

$Al_xFe_ySi_z$ phase than Fe_2Al_5 [21]. However, Al-Mo-modified coating showed a contradictory trend in layer thickness relative to Al-Si-modified and Al-Si-Mo-modified coatings. The coating products showed an increase in layer thickness as the aluminizing time increases from 4 h to 6 h with 59.89 µm (inner: 10.12 ± 3.51 µm + outer: 49.77 ± 11.32 µm) and 88.00 µm (inner: 19.55 ± 6.43 µm + outer: 68.45 ± 11.26 µm), respectively (Figure 3(c)).

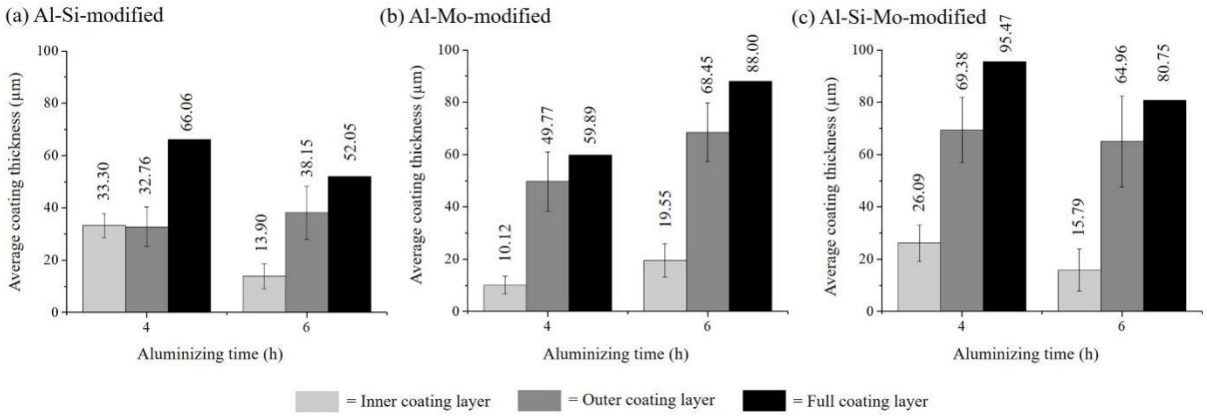

Figure 3. Comparison of coating layer thickness on 304 stainless steel after aluminizing at 650 ºC for 4 h and 6 h: (a) Al-Si-modified coating, (b) Al-Mo-modified coating and (c) Al-Si-Mo-modified coating.

Mechanical properties of the coatings. The mechanical properties of the coating layers were assessed by a micro-hardness test. Figure 4 shows the Vickers microhardness profiles performed on the surface of modified-aluminide coatings after 4 h and 6 h of aluminizing. The hardness after 4 h aluminizing of Al-Si-modified and Al-Mo-modified coatings were 33.20 HV and 42.47 HV, respectively. The hardness values of those coatings increased as the aluminizing time increased to 6 h with 66.60 HV and 60.33 HV, respectively. However, those results contradicted with Al-Si-Mo-modified coating. The Al-Si-Mo-modified coating showed a decline in hardness value with aluminizing time. The micro-hardness of the coating layer was related to its constituent phases [14]. A high hardness increment was obtained attributed to the formation of FeAl intermetallic during the coating process [36]. The existence of phases, such as Fe_2Al_5 and $FeAl_2$ might contribute to a high hardness value due to its properties as a hard intermetallic compound [14,21].

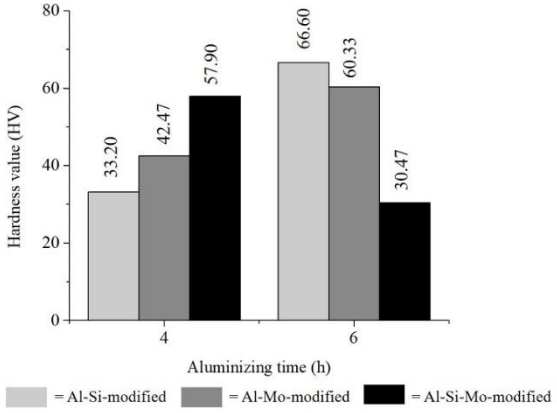

Figure 4. Vickers microhardness test of all aluminide coated 304 stainless steel

The overall results revealed that the addition of Si and Mo into the coating by a slurry aluminizing process modified the properties of iron-aluminide coating layer on the 304 austenitic stainless steel. The appearance of the additional intermetallic phase of Al_7Fe_2Si was detected by the addition of 10 wt. % Si into the coating composition. While the additional phase of MoO_3 was identified by the modified aluminide coating with the addition of 5 -10 wt.% Mo. Future work is needed to strengthen the finding of this study. The modified slurry aluminide coatings were aimed for oxidation and hot corrosion test under high temperature conditions. A dense and homogenous FeAl-base intermetallic coating layer formed on substrate surfaces was believed to protect the inner alloy substrate from serious degradation and material loss. The improvement of the high temperature oxidation resistance of aluminized stainless steel was caused by the formation of the protective Al_2O_3 layer on the substrate surface [14]. A study by Soleimani et al. (2016) has found that aluminide coating significantly improves the oxidation resistance of P91 steel and AISI 304SS against solar salt at 600 ºC for 1700 h due to the formation of $Na(Fe, Al)O_2$ at the surface of the coating, which prevents corrosion attack on the substrate [13]. Shirvani et al. (2020) also mentioned that the addition of Si into the aluminide coating has the ability to change the degradation mechanism of the protective surface oxide layer. According to the study, the presence of Si as a metallic alloying element in the coating layer improves the protective properties of the forming oxide layer at high temperatures due to the formation of Al_2O_3-SiO_2 [20].

Conclusion

The Si-, Mo- and Si-Mo-modified aluminized coatings were successfully applied on the 304 stainless steel through the slurry process at 650 ºC for 4 h and 6 h. The morphology, elemental composition, phase analysis and hardness of the coatings were examined. The microstructure of the aluminide coatings consists of a double-layer structure made up of the outer diffusion layer and inner interdiffusion layer. The aluminizing was found to develop a coating layer primarily consisting of Fe_2Al_5 and $FeAl_3$. The additional FeAlSi intermetallic (Al_7Fe_2Si) and MoO_3 phases were found in the modified aluminide coating layer. The formation of a continuous and dense FeAl-rich inner layer on Si-Mo-modified coating after 4 h of aluminizing contributes to a high coating hardness. While the addition of 10% of Si into the coating effectively enhanced the coating hardness after 6 h of aluminizing by the formation of a double coating layer composed of Al-rich oxide (Al_2O_3) and inner FeAl-base intermetallic layer.

Acknowledgements

This work was supported by the Ministry of Higher Education Malaysia via Fundamental Research Grant Scheme, FRGS with grant number; FRGS/1/2018/TK05/USM/03/3.

Author Contributions

Syamimi Abu Kassim: Investigation, Methodology, Writing - original draft. Nur Muzirah Md Shukri: Investigation, Visualization, Methodology. Anasyida Abu Seman: Conceptualization. Tuti Katrina Abdullah: Supervision, Conceptualization, Writing - review & editing, Methodology, Funding acquisition.

Disclosure of Conflict of Interest

The authors declare that they have no known competing financial interests or personal relationships that could have appeared to influence the work reported in this paper.

Compliance with Ethical Standards

The work is compliant with ethical standard.

References

[1] Boulesteix, C., & Grégoire, B. & Pedraza, F. (2017). Oxidation performance of repaired aluminide coatings on austenitic steel substrates. *Surf. Coatings Technol.* 326 224–237.

[2] Huang, J., Lu, J., Zhang, X., Yang, Z., Zhou, Y., Yang, Z., Dang, Y. & Yuan, Y. (2019). Preparation and Characterization of Slurry Aluminide Coating on TP347H FG Stainless Steel. *Metall. Mater. Trans. A Phys. Metall. Mater. Sci.* 50 (8) 3776–3784.

[3] Promdirek, P., Boonpensin, M. & Rojasawasatien, T. (2015). Improvement of slurry aluminide coating on ferritic stainless steel AISI430 for high-temperature oxidation resistance. *Key Eng. Mater.* 658 86–90.

[4] Pedraza, F., Proy, M., Boulesteix, C., Krukovskyi, P. & Metel, M. (2016). Slurry aluminizing of IN-800HT austenitic stainless steel and pure nickel. Correlations between experimental results and modelling of diffusion. *Mater. Corros*. 67 (10) 1059–1067.

[5] Lu, J., Dang, Y., Huang, J., Zhou, Y., Yang, Z., Yan, J., Yuan, Y. & Gu, Y. (2019). Preparation and characterization of slurry aluminide coating on Super304H boiler tube in combination with heat-treatment process. *Surf. Coatings Technol.* 370 (136) 97–105.

[6] Lu, J., Huang, J., Wang, J., Yang, Z. & Gu, Y. (2021). Long-term degradation behavior of slurry aluminide coating on Super304H stainless steel at 650 °C. *Corros. Sci.* 178 (136) 109054.

[7] Bauer, J. T., Montero, X. & Galetz, M.C. (2020). Fast heat treatment methods for al slurry diffusion coatings on alloy 800 prepared in air. *Surf. Coatings Technol.* 381 125140.

[8] Cheng, W.J. & Wang, C.J. (2011). Effect of silicon on the formation of intermetallic phases in aluminide coating on mild steel. *Intermetallics*. 19 (10) 1455–1460.

[9] Dong, J., Sun, Y. & He, F. (2019). Formation mechanism of multilayer aluminide coating on 316L stainless steel by low-temperature pack cementation. *Surf. Coatings Technol.* 375 833–838.

[10] Bauer, J.T., Montero, X., Schütze, M. & Galetz, M.C. (2016). Innovative slurry coating concepts for aluminizing of an austenitic steel in chlorine and sulfur containing atmosphere. *Surf. Coatings Technol.* 285 179–186.

[11] Sun, Y., Dong, J., Zhao, P. & Dou, B. (2017). Formation and phase transformation of aluminide coating prepared by low-temperature aluminizing process. *Surf. Coatings Technol.* 330 234–240.

[12] Mahini, S., Khameneh Asl, S., Rabizadeh, T. & Aghajani, H. (2020). Effects of the pack Al content on the microstructure and hot corrosion behavior of aluminide coatings applied on Inconel-600. *Surf. Coatings Technol.* 397 125949.

[13] Soleimani Dorcheh, A. & Galetz, M.C. (2016). Slurry aluminizing: A solution for molten nitrate salt corrosion in concentrated solar power plants. *Sol. Energy Mater. Sol. Cells.* 146 8–15.

[14] Zarei, F., Nuranian, H. & Shirvani, K. (2020). Characterization, growth kinetics and high-temperature oxidation behavior of aluminide coating formed on HH309 stainless steel by casting and subsequent heat treatment. *Intermetallics.* 120 106742.

[15] Yang, R., Wu, Y., Wu, Q., Li, S., Ma, Y. & Gong, S. (2012). Microstructure and oxidation behavior of modified aluminide coating on Ni3Al-based single crystal superalloy. *Chinese J. Aeronaut.* 25 (5) 825–830.

[16] Tavakoli Targhi, V., Omidvar, H., Sharifianjazi, F. & Pakseresht, A. (2020). Hot corrosion behavior of aluminized and Si-modified aluminized coated IN-738LC produced by a novel hot-dip process. *Surfaces and Interfaces.* 21 100599.

[17] Yavorska, M. & Sieniawski, J. (2011). Oxidation behaviour of platinum modified aluminide coatings deposited by CVD method on nickel-based superalloys under air atmosphere. *J. Achiev. Mater. Manuf. Eng.* 46 (2) 204–210.

[18] Jiang, C. Y., Yang, Y. F., Zhang, Z. Y., Bao, Z. B., Chen, M. H., Zhu, S. L. & Wang F. H. (2018). A Zr-doped single-phase Pt-modified aluminide coating and the enhanced hot corrosion resistance. *Corros. Sci*. 133 406–416.

[19] Pang, J., Wang, W. & Zhou, C. (2016). Microstructure evolution and oxidation behavior of B modified $MoSi_2$ coating on Nb-Si based alloys. *Corros. Sci.* 105 1–7.

[20] Zarei, F., Nuranian, H. & Shirvani, K. (2020). Effect of Si addition on the microstructure and oxidation behaviour of formed aluminide coating on HH309 steel by cast-aluminizing. *Surf. Coatings Technol.* 394 125901.

[21] Troysi, F. D. & Brito, P. P. (2020). Development and characterization of an iron aluminide coating on mild steel substrate obtained by friction surfacing and heat treatment. *Int. J. Adv. Manuf. Technol.* 111 (10) 2569–2576.

[22] Bermejo Sanz, J., Roussel García, R., Kolarik, V., Del M. & Juez Lorenzo M. (2017). Influence of the Slurry Thickness and Heat Treatment Parameters on the Formation of Aluminium Diffusion Coating. *Oxid. Met.* 88 (2) 179–190.

[23] Audigié, P., Encinas-Sánchez, V., Rodríguez, S., Pérez, F.J. & Agüero, A. (2020). High temperature corrosion beneath carbonate melts of aluminide coatings for CSP application. *Sol. Energy Mater. Sol. Cells.* 210 110514.

[24] Grégoire, B., Bonnet, G. & Pedraza, F. (2019). Mechanisms of formation of slurry aluminide coatings from Al and Cr microparticles. *Surf. Coatings Technol.* 359 323–333.

[25] Goral, M., Ochal, K., Kubaszek, T. & Drajewicz, M. (2020). The influence of deposition technique of aluminide coatings on oxidation resistance of different nickel superalloys. *Mater. Today Proc.* 33 1746–1751.

[26] Zare Mohazabie, M. S. & Shahriari Nogorani, F. (2019). The addition of zirconium to aluminide coatings: The effect of the aluminide growth mode. *Surf. Coatings Technol.* 378 125066.

[27] Fu, Q. G., Zhang, J. P., Zhang, Z. Z., Li, H. J. & Sun, C. (2013). SiC-$MoSi_2$/ZrO_2-$MoSi_2$ coating to protect C/C composites against oxidation. *Trans. Nonferrous Met. Soc. China English Ed.* 23 (7) 2113–2117.

[28] Wang, C. C., Li, K. Z., He, D. Y. & Shi X. H. (2020). Oxidation behavior of plasma-sprayed $MoSi_2$-Yb_2O_3 composite coating at 1700 °C. *Ceram. Int.* 46 (7) 9538–9547.

[29] Shirvani, K., Saremi, M., Nishikata, A. & Tsuru, T. (2003). Electrochemical study on hot corrosion of Si-modified aluminide coated In-738LC in Na_2SO_4-20 wt.% NaCl melt at 750 °C. *Corros. Sci.* 45 (5) 1011–1021.

[30] Boulesteix, C., Kolarik, V. & Pedraza, F. (2018). Steam oxidation of aluminide coatings under high pressure and for long exposures. *Corros. Sci.* 144 328–338.

[31] Yener, T., Erdogan, A., Gök, M. S. & Zeytin, S. (2021). Formation, characterization, and wear behavior of aluminide coating on mirrax® ESR steel by low-temperature aluminizing process. *J. Tribol.* 143 (1) 011703-1.

[32] Cheng, W. J. & Wang, C. J. (2010). Observation of high-temperature phase transformation in the Si-modified aluminide coating on mild steel using EBSD. *Mater. Charact.* 61 (4) 467–473.

[33] Chang, Y. Y., Tsaur, C. C. & Rock, J. C (2006). Microstructure studies of an aluminide coating on 9Cr-1Mo steel during high temperature oxidation. *Surf. Coatings Technol.* 200 (22-23 special issue) 6588–6593.

[34] Cheng, W. J. & Wang, C. J. (2009). EBSD study of crystallographic identification on Fe-Al-Si lntermetallic phases in aluminide coatings on mild steels. *Adv. Mater. Res.* 79–82 907–910.

[35] Zhang, Y., Li, Y. & Bai, C. (2017). Microstructure and oxidation behavior of Si–MoSi2 functionally graded coating on Mo substrate. *Ceram. Int.* 43 (8) 6250–6256.

[36] Yener, T. (2019). Low temperature aluminising of Fe-Cr-Ni super alloy by pack cementation. *Vacuum.* 162 114–120.